Lab on a Chip

RSC Publishing

COMMUNICATION

View Article Online
View Journal | View Issue

Self-assembled DNA tetrahedral optofluidic lasers with precise and tunable gain control†

Cite this: *Lab Chip*, 2013, **13**, 3351

Received 22nd May 2013,
Accepted 24th June 2013

DOI: 10.1039/c3lc50629k

www.rsc.org/loc

Qiushu Chen,‡[a] Huajie Liu,‡[b] Wonsuk Lee,‡[ac] Yuze Sun,[a] Dan Zhu,[b] Hao Pei,[b] Chunhai Fan*[b] and Xudong Fan*[a]

We have applied self-assembled DNA tetrahedral nanostructures for the precise and tunable control of the gain in an optofluidic fluorescence resonance energy transfer (FRET) laser. By adjusting the ratio of the donor and the acceptor attached to the tetrahedral vertices, 3.8 times reduction in the lasing threshold and 28-fold enhancement in the lasing efficiency were demonstrated. This work takes advantage of the self-recognition and self-assembly capabilities of biomolecules with well-defined structures and addressability, enabling nano-engineering of the laser down to the molecular level.

With the unparalleled ability of programmable hybridization through unique base pair recognition, DNA holds a great promise as a powerful material for the construction of a wide range of highly uniform and well defined nanostructures.[1–5] In particular, DNA tetrahedral nanostructures[6–8] have received great interest due to their synthetic simplicity, mechanical rigidity, structural stability, and modification versatility. Based on these unique features of DNA tetrahedra, a variety of applications including sensors,[9,10] logic gates,[11] fluorescent nanotags,[12] and nanocages for protein encapsulation and drug delivery have been developed.[13,14] The size and geometry of DNA tetrahedra are also highly tunable and can be readily adjusted by varying the length and conformation of the edge strands.[15] Hence, it is possible to design dynamic tetrahedral nanostructures that can finely manipulate the optical and electrical interactions of functional molecules anchored on the DNA tetrahedra.[11]

Indeed, DNA nanostructures offer versatile ways for the anchoring of (bio)molecules and nanoparticles with high addressability and a nanoscale resolution of 6 nm. By exploiting such a property, Kuzyk *et al.* employed a DNA origami structure to precisely assemble gold nanoparticles into chiral plasmonic nanostructures with tailored optical responses.[16] More recently, Acuna *et al.* designed a plasmonic nanoantenna structure that site-specifically attached gold nanoparticles to form hotspots for fluorescence enhancement.[17] Likewise, DNA tetrahedra provide an ideal platform for the precise anchoring of metal nanoparticles for optical applications.[18,19]

Here we demonstrate that tetrahedral DNA nanostructures can be employed to precisely control and finely tune the gain of an optofluidic laser. Optofluidic lasers are an emerging area that integrates microfluidics with a laser cavity and gain medium in liquid, and provides a promising technology platform for the development of on-chip tunable laser sources and highly sensitive biochemical sensors.[20–26] The laser gain is one of the most important parameters, which determines many other laser characteristics such as lasing threshold, efficiency and output power.[27] The combination of the aforementioned biological nano-engineering concept and the optofluidic laser takes advantage of the self-recognition and self-assembly capabilities of biomolecules with sub-nanometer accuracy, their well-defined structures and stoichiometry, thus enabling the precise control and tuning of the laser characteristics at the molecular level.

In the current work, the gain medium of the optofluidic laser consisted of a fluorescence resonance energy transfer (FRET) pair, Cy3 (donor) and Cy5 (acceptor), attached to the vertex of the DNA tetrahedron. Cy3 acts as an antenna to collect the excitation light and then transfers the energy through FRET for Cy5 to lase. Optimization of the Cy3 and Cy5 arrangement on the DNA tetrahedron resulted in a significant improvement in the lasing characteristics with a 3.8-fold reduction in the lasing threshold and 28-fold increase in the lasing efficiency. A theoretical analysis was also carried out to elucidate the control and tuning capability of the DNA nanostructures.

DNA tetrahedron preparation and characterization

We used two types of DNA tetrahedra. 1Cy3–3Cy5 has 1 Cy3 molecule and 3 Cy5 molecules attached to each tetrahedron,

[a]*Department of Biomedical Engineering, University of Michigan, 1101 Beal Ave., Ann Arbor, MI 48109, United States. E-mail: xsfan@umich.edu*
[b]*Division of Physical Biology, and Bioimaging Center, Shanghai Synchrotron Radiation Facility, Shanghai Institute of Applied Physics, Chinese Academy of Sciences, Shanghai 201800, China. E-mail: fchh@sinap.ac.cn*
[c]*Department of Electrical Engineering and Computer Science, University of Michigan, 1301 Beal Avenue, Ann Arbor, MI 48109, United States*
† Electronic supplementary information (ESI) available. See DOI: 10.1039/c3lc50629k
‡ Equal contribution.

whereas 3Cy3–1Cy5 has 3 Cy3 molecules and 1 Cy5 molecule attached to each tetrahedron (Fig. 1(A)). Each type of tetrahedron was formed by mixing four 32-base single-stranded DNA (Table S1, ESI†) in a stoichiometric ratio (1 μM) in 1 × TM–Mg buffer (20 mM Tris-HCl, 20 mM $MgCl_2$, pH 8.0 adjusted by acetic acid). After the formation of the tetrahedral nanostructure, each arm has 10 bases with a length of 3.4 nm. The solution was heated to 95 °C for 8 min and then quickly cooled to 4 °C. The prepared DNA tetrahedra were concentrated using a 100 kD Centricon spin-filter (Millipore). The DNA tetrahedra were characterized and purified with a native 10% polyacrylamide gel (PAGE), which was run at 4 °C and stained with SYBR Gold (see Fig. S1, ESI†). The formation of the purified product was further confirmed by high-performance liquid chromatography (HPLC) (see Fig. 1(B)). Fluorescence tests were carried out using an Edinburgh Instruments F900 spectrofluorometer (see Fig. 1(C)), which clearly showed the presence of FRET between Cy3 and Cy5. Furthermore, comparison of Curve 2 and 3 with Curve 1 suggests that the tetrahedra with multiple donors (3Cy3–1Cy5) have higher acceptor excitation (and hence emission) than those with multiple acceptors (1Cy3–3Cy5).

Optofluidic laser

The laser used in our experiment was based on the optofluidic ring resonator (OFRR) (Fig. 2).[28,29] The OFRR is a piece of a thin-walled glass capillary. The circular-shaped OFRR cross section supports the high-Q whispering gallery mode (WGM) circulating along the ring resonator circumference. The WGM has an evanescent field inside the core to provide the optical feedback for the laser gain medium (such as Cy5) to lase.

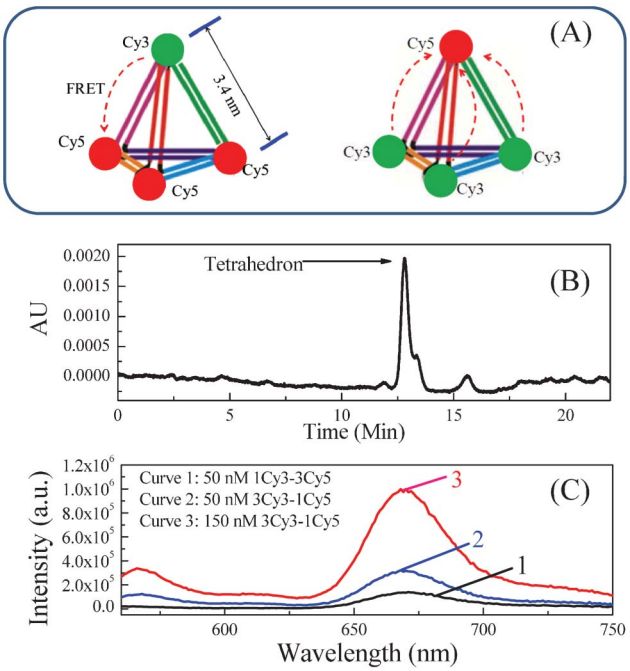

Fig. 1 (A) DNA tetrahedra used in the optofluidic FRET laser by mixing the four 32-base single-stranded DNA listed in Table S1, ESI.† Left: 1Cy3–3Cy5, molar ratio between Cy3 (donor) and Cy5 (acceptor) was 1 : 3. Right: 3Cy3–1Cy5, molar ratio between Cy3 (donor) and Cy5 (acceptor) was 3 : 1. (B) Confirmation of the purified DNA tetrahedra with HPLC. The peak with an arrow corresponds to the formed DNA tetrahedra. (C) Fluorescent analysis of DNA tetrahedra labeled with the Cy3–Cy5 FRET pair (λ_{ex} = 555 nm). Curve 1 is for 50 nM of 1Cy3–3Cy5, whereas Curve 2 and 3 are for 50 nM and 150 nM of 3Cy3–1Cy5, respectively.

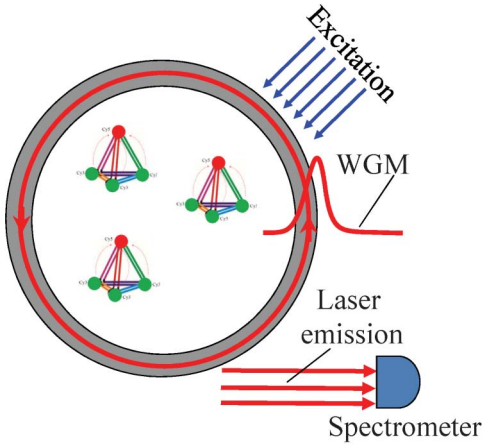

Fig. 2 Experimental setup. The whispering gallery mode (WGM) supported by the cross section of the capillary based optofluidic ring resonator (OFRR) provides the optical feedback for Cy5 (acceptor) to lase. The laser was excited by an external OPO within the Cy3 (donor) absorption band (518 nm).

The fabrication process of the OFRR was the same as that in our earlier work.[28,29] The OFRR had an outer diameter of 90 μm and a wall thickness below 2 μm. During the experiment, we used 15 μM of the 1Cy3–3Cy5 tetrahedron and 45 μM of the 3Cy3–1Cy5 tetrahedron, which ensured that both samples had the same concentration of the lasing medium (Cy5), thus eliminating the concentration dependence in the lasing parameters such as the lasing threshold[30,31] and allowing us to compare the two laser systems directly. The sample in 1 × TM–Mg buffer was withdrawn into the capillary by a syringe pump. The solution was excited by a pulsed optical parametric oscillator (OPO, 5 ns pulse width and 20 Hz repetition rate) within the Cy3 (donor) absorption band (518 nm). Cy5 (acceptor) was subsequently excited to lase through the FRET process, and its laser emission was collected by a multimode optical fiber and sent to a spectrometer for analysis (see Fig. 2).

DNA tetrahedra-controlled optofluidic FRET lasers

The experiment results show that DNA tetrahedra with different donor-to-acceptor ratios have different laser characteristics in the optofluidic laser system. The performance of the optofluidic laser is significantly improved by optimization of the donor–acceptor arrangement. Fig. 3 shows the lasing spectrum of both 1Cy3–3Cy5 and 3Cy3–1Cy5 when pumped near or well above the threshold. Laser modes are observed in the wavelength range within the acceptor (Cy5) emission band. Note that the longest lasing wavelength for the 3Cy3–1Cy5 system is around 740 nm, red-shifted from that for the 1Cy3–3Cy5 system. This red-shift is strong evidence that the 3Cy3–1Cy5 system has a larger gain.[30,31]

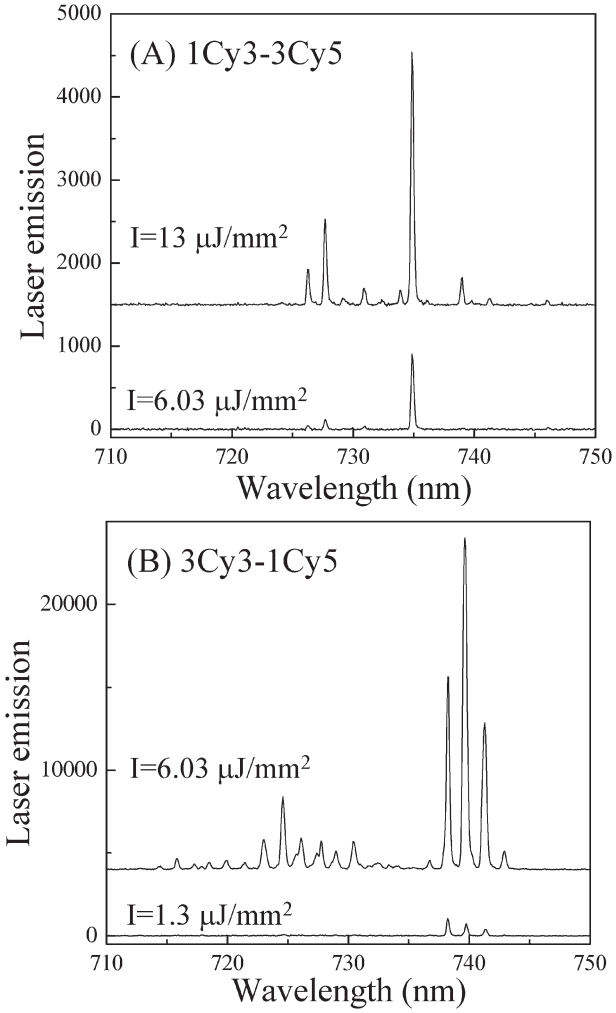

Fig. 3 Optofluidic laser spectra from Cy5 for 1Cy3–3Cy5 (A) and 3Cy3–1Cy5 (B) at different pump energy densities. Concentration was 15 μM and 45 μM for (A) and (B), respectively. Other conditions such as buffer, temperature, and flow rate remained the same.

Indeed, such a difference in the gain is quantitatively reflected in the lasing threshold of the 3Cy3–1Cy5 system, as shown in Fig. 4, which is 3.8 times lower than that of the 1Cy3–3Cy5 system (1.18 μJ mm^{-2} *vs.* 4.5 μJ mm^{-2}). Furthermore, according to Fig. 4, the lasing differential efficiency (slope of laser emission *vs.* pump intensity) is 28-fold enhanced in the 3Cy3–1Cy5 system, in comparison with that in the 1Cy3–3Cy5 system, suggesting that efficient photon conversion can be achieved by simply re-arranging the molar ratio between the donor and the acceptor.

A theoretical analysis was performed to account for the drastic difference between the two tetrahedral configurations. The excitation of the laser gain medium (*i.e.*, Cy5) comes from the excitation of the donor (Cy3), which later transfers to the acceptor (Cy5) *via* FRET. The rate equations for the 1Cy3–3Cy5 system can be approximately expressed as:

$$\frac{dn_{Cy3,1}}{dt} = R_p - k_{Cy3}\cdot n_{Cy3,1} - 3k_{FRET}\cdot n_{Cy3,1} \quad (1)$$

$$\frac{dn_{Cy5,1}}{dt} = k_{FRET}\cdot n_{Cy3,1} - k_{Cy5}\cdot n_{Cy5,1} \quad (2)$$

where $n_{Cy3,1}$ and $n_{Cy5,1}$ are the fraction of Cy3 and Cy5 molecules in the excited state, respectively. k_{Cy3} and k_{Cy5} are the decay rates for Cy3 and Cy5 at the excited state, respectively. k_{FRET} is the energy transfer rate. R_p is the excitation rate for Cy3, *i.e.*:

$$R_p \propto n_{Cy3,total}\cdot\sigma_{Cy3}\cdot I_p, \quad (3)$$

where $n_{Cy3,total}$, σ_{Cy3}, and I_p are the total number of Cy3 molecules, the Cy3 absorption cross section, and the external pump light intensity, respectively. Under the steady-state approximation, the excitation of Cy5 is:

$$n_{Cy5,1} \propto \frac{E}{3}\cdot n_{tetrahedron}\cdot\sigma_{Cy3}\cdot I_p, \quad (4)$$

where $n_{tetrahedron}$ is the number of tetrahedra. E is the FRET efficiency:

$$E = \frac{3k_{FRET}}{k_{Cy3}+3k_{FRET}} = \frac{3R_0{}^6}{r^6+3R_0{}^6}, \quad (5)$$

where R_0 is the Förster distance for Cy3 and Cy5. r is the distance between Cy3 and Cy5. Similarly, the excitation of Cy5 in the 3Cy3–1Cy5 system is given by:

$$n_{Cy5,1} \propto 3E'\cdot n_{tetrahedron}\cdot\sigma_{Cy3}\cdot I_p, \quad (6)$$

where

$$E' = \frac{k_{FRET}}{k_{Cy3}+k_{FRET}} = \frac{R_0{}^6}{r^6+R_0{}^6}. \quad (7)$$

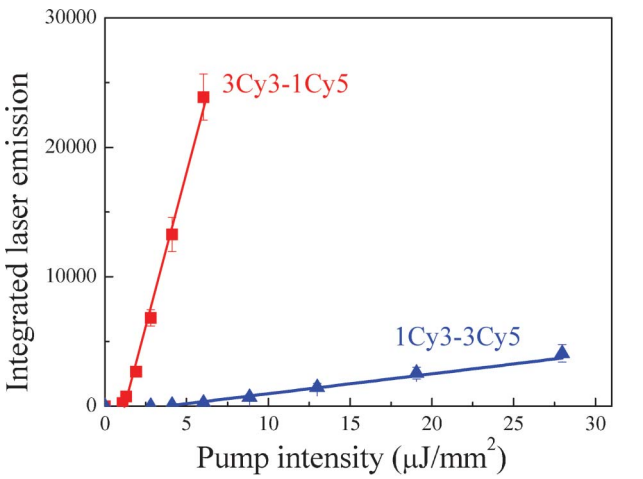

Fig. 4 Spectrally integrated laser emission as a function of the pump intensity for 1Cy3–3Cy5 and 3Cy3–1Cy5 lasers. The lasing threshold was 4.5 μJ mm^{-2} and 1.18 J mm^{-2} for 1Cy3–3Cy5 and 3Cy3–1Cy5, respectively. The laser differential efficiency was 174 mm^2 μJ^{-1} and 4770 mm^2 μJ^{-1} for 1Cy3–3Cy5 and 3Cy3–1Cy5, respectively. Solid lines are the linear fit above the lasing threshold. Spectral integration took place between 683 nm and 756 nm. Error bars were obtained from 5 measurements.

Given R_0 = 6 nm and r = 3.4 nm in our current system, E and E' are calculated to be 99% and 97%, respectively, for 1Cy3–3Cy5 and 3Cy3–1Cy5. Since the lasing threshold is directly related to the fraction of gain medium molecules (Cy5) in the excited state, the lasing threshold for 3Cy3–1Cy5 is thus calculated to be 8.8 times lower than for 1Cy3–3Cy5, qualitatively agreeing with the experimental results. The quantitative discrepancy between the experiment result and the theoretical analysis might result from the optical loss in the Cy5 emission caused by the extra Cy3 absorption in 3Cy3–1Cy5, as it has 9 times more Cy3.[30,32]

The experimental observation and the theoretical study presented above introduce two ways of laser gain control in an optofluidic laser. The first method utilizes the DNA scaffold technique to explore the donor-to-acceptor ratio for different gain characteristics. When an acceptor is surrounded by multiple donors in proximity, a high excitation efficiency of the acceptor can be achieved in comparison with the case where only one donor is available. More generally, a hierarchical structure can be used for an even higher excitation efficiency, where the acceptor is excited *via* FRET from multiple intermediate molecules, each of which is, in turn, excited *via* FRET from multiple donors. The second method is to adjust the distance between donor and acceptor through flexible or reconfigurable DNA structures to control the FRET efficiency and hence the gain medium excitation efficiency. In the DNA tetrahedron case, the length of the tetrahedron edge can be finely tuned by varying the number of base pairs and/or the conformational change of the embedded functional domains.[11] These two methods can work in tandem to provide a better control over the laser characteristics.

In conclusion, DNA tetrahedra were used to control the optofluidic laser through a FRET acceptor–donor arrangement. This work synergizes flexible, programmable, and cell-permeable DNA tetrahedral nanostructures with the optofluidic laser technology, which has a high sensitivity and handles nano-liter sized sample volumes with ease. Therefore, a broad range of applications can be explored in the area of novel photonic devices, bio-nanotechnology, biochemical sensing, and biomedical research.

Acknowledgements

This work was supported by the National Science Foundation under ECCS-1045621 and CBET-1037097, and by the National Basic Research Program of China (973 program, 2013CB933800, 2013CB932803) and the National Natural Science Foundation of China (Grant No. 21227804).

References

1 N. C. Seeman, *Nature*, 2003, **421**, 427–431.
2 A. V. Pinheiro, D. Han, W. M. Shih and H. Yan, *Nat. Nanotechnol.*, 2011, **6**, 763–772.
3 S. J. Tan, M. J. Campolongo, D. Luo and W. Cheng, *Nat. Nanotechnol.*, 2011, **6**, 268–276.
4 T. Tørring, N. V. Voigt, J. Nangreave, H. Yan and K. V. Gothelf, *Chem. Soc. Rev.*, 2011, **40**, 5636–5646.
5 N. Y. Wong, H. Xing, L. H. Tan and Y. Lu, *J. Am. Chem. Soc.*, 2013, **135**, 2931–2934.
6 R. P. Goodman, I. A. T. Schaap, C. F. Tardin, C. M. Erben, R. M. Berry, C. F. Schmidt and A. J. Turberfield, *Science*, 2005, **310**, 1661–1665.
7 R. P. Goodman, M. Heilemann, S. Doose, C. M. Erben, A. N. Kapanidis and A. J. Turberfield, *Nat. Nanotechnol.*, 2008, **3**, 93–96.
8 C. Zhang, M. Su, Y. He, Y. Leng, A. E. Ribbe, G. Wang, W. Jiang and C. Mao, *Chem. Commun.*, 2010, **46**, 6792–6794.
9 H. Pei, N. Lu, Y. Wen, S. Song, Y. Liu, H. Yan and C. Fan, *Adv. Mater.*, 2010, **22**, 4754–4758.
10 Y. Wen, H. Pei, Y. Shen, J. Xi, M. Lin, N. Lu, X. Shen, J. Li and C. Fan, *Sci. Rep.*, 2012, **2**, 867.
11 H. Pei, L. Liang, G. Yao, J. Li, Q. Huang and C. Fan, *Angew. Chem., Int. Ed.*, 2012, **51**, 9020–9024.
12 H. Özhalıcı-Ünal and B. A. Armitage, *ACS Nano*, 2009, **3**, 425–433.
13 C. M. Erben, R. P. Goodman and A. J. Turberfield, *Angew. Chem., Int. Ed.*, 2006, **45**, 7414–7417.
14 J. Li, H. Pei, B. Zhu, L. Liang, M. Wei, Y. He, N. Chen, D. Li, Q. Huang and C. Fan, *ACS Nano*, 2011, **5**, 8783–8789.
15 N. Mitchell, R. Schlapak, M. Kastner, D. Armitage, W. Chrzanowski, J. Riener, P. Hinterdorfer, A. Ebner and S. Howorka, *Angew. Chem., Int. Ed.*, 2009, **48**, 525–527.
16 A. Kuzyk, R. Schreiber, Z. Fan, G. Pardatscher, E.-M. Roller, A. Högele, F. C. Simmel, A. O. Govorov and T. Liedl, *Nature*, 2012, **483**, 311–314.
17 G. P. Acuna, F. M. Möller, P. Holzmeister, S. Beater, B. Lalkens and P. Tinnefeld, *Science*, 2012, **338**, 506–510.
18 A. J. Mastroianni, S. A. Claridge and A. P. Alivisatos, *J. Am. Chem. Soc.*, 2009, **131**, 8455–8459.
19 W. Yan, L. Xu, C. Xu, W. Ma, H. Kuang, L. Wang and N. A. Kotov, *J. Am.Chem. Soc.*, 2012, **134**, 15114–15121.
20 X. Fan and I. M. White, *Nat. Photonics*, 2011, **5**, 591–597.
21 H. Schmidt and A. R. Hawkins, *Nat. Photonics*, 2011, **5**, 598–604.
22 D. Psaltis, S. R. Quake and C. Yang, *Nature*, 2006, **442**, 381–386.
23 C. Monat, P. Domachuk and B. J. Eggleton, *Nat. Photonics*, 2007, **1**, 106–114.
24 W. Lee and X. Fan, *Anal. Chem.*, 2012, **84**, 9558–9563.
25 T. Wienhold, F. Breithaupt, C. Vannahme, M. B. Cristiansen, W. Dorfler, A. Kristensen and T. Mappes, *Lab Chip*, 2012, **12**, 3734–3739.
26 Q. Chen, X. Zhang, Y. Sun, M. Ritt, S. Sivaramakrishnan and X. Fan, *Lab Chip*, 2013, **13**, 2679.
27 A. E. Siegman, *Lasers*, University Science Books, Sausalito, CA, 1986.
28 Y. Sun, S. I. Shopova, C.-S. Wu, S. Arnold and X. Fan, *Proc. Natl. Acad. Sci. U. S. A.*, 2010, **107**, 16039–16042.
29 Y. Sun and X. Fan, *Angew. Chem., Int. Ed.*, 2012, **51**, 1236–1239.
30 H.-J. Moon, Y.-T. Chough and K. An, *Phys. Rev. Lett.*, 2000, **85**, 3161–3164.
31 S. Lacey, I. M. White, Y. Sun, S. I. Shopova, J. M. Cupps, P. Zhang and X. Fan, *Opt. Express*, 2007, **15**, 15523–15530.
32 Z. Li and D. Psaltis, *Microfluid. Nanofluid.*, 2008, **4**, 145–158.

